JACS
JOURNAL OF THE AMERICAN CHEMICAL SOCIETY

ARTICLE

pubs.acs.org/JACS

Epimeric Monosaccharide−Quinone Hybrids on Gold Electrodes toward the Electrochemical Probing of Specific Carbohydrate−Protein Recognitions

Xiao-Peng He,[†,‡] Xiu-Wen Wang,[†] Xiao-Ping Jin,[†] Hao Zhou,[†] Xiao-Xin Shi,[‡] Guo-Rong Chen,[†] and Yi-Tao Long*[,†]

[†]Key Laboratory for Advanced Materials and Institute of Fine Chemicals, and [‡]School of Pharmacy, East China University of Science and Technology, 130 Meilong Road, Shanghai, People's Republic of China

Supporting Information

ABSTRACT: Carbohydrates represent one of the most significant natural building blocks, which govern numerous critical biological and pathological processes through specific carbohydrate−receptor interactions on the cell surface. We present here a new class of electrochemical probes based on gold surface-coated epimeric monosaccharide−quinone hybrids toward the ingenious detection of specific epimeric carbohydrate−protein interactions. Glucose and galactose, which represent a pair of natural monosaccharide C4 epimers, were used to closely and solidly conjugate with the 1,4-dimethoxybenzene moiety via a single C−C glycosidic bond, followed by the introduction of a sulfhydryl anchor. The functionalized aryl *C*-glycosides were sequentially coated on the gold electrode via the self-assembled monolayer (SAM) technique. X-ray photoelectron spectroscopy (XPS) was used to confirm the SAM formation, by which different binding energies (BE) between the glucosyl and the galactosyl SAMs on the surface, probably rendered by their epimeric identity, were observed. The subsequent electrochemical deprotection process readily furnished the surface-confined quinone/hydroquinone redox couple, leading to the formation of electrochemically active epimeric monosaccharide−quinone SAMs on the gold electrode. Cyclic voltammetry (CV) and differential pulse voltammetry (DPV) used for the detection of specific sugar−lectin interactions indicated that the addition of specific lectin to the corresponding monosaccharide−quinone surface, i.e., concanavalin A (Con A) to the glucosyl SAM and peanut agglutinin (PNA) to the galactosyl SAM, resulted in an obvious decrease in peak current, whereas the addition of nonspecific lectins to the same SAMs gave very minor current variations. Such data suggested our uniquely constructed gold surface coated by sugar−quinone hybrids to be applicable as electrochemical probes for the detection of specific sugar−protein interactions, presumably leading to a new electrochemistry platform toward the study of carbohydrate-mediated intercellular recognitions.

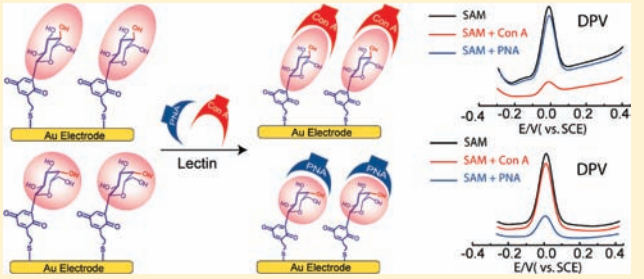

Carbohydrates are ubiquitously distributed in all living organisms that exist in nature, governing a wide spectrum of pivotal biological and pathological events including cell−cell recognition, signal transduction, autoimmune stimulation, tumor metastasis, etc. by generating multivalent interactions with corresponding carbohydrate receptors on cells.[1−5] Meanwhile, since the diverse "sugar chains" that are pervasive on the cell surface are concomitantly varied by cellular malignancy, development, or differentiation, the real-time and accurate probing of specific carbohydrate−receptor interactions that are associated with these dynamic cellular events became crucial for early-state disease diagnosis. However, natural carbohydrates as well as their receptors lack measurable signals due to the absence of "reporters" such as a fluorophore. To tackle this issue, numerous analytical methods including NMR or fluorescence spectroscopy, isothermal calorimetry, and quartz crystal microbalance (QCM) and surface plasmon resonance (SPR) techniques have been developed in the past decade, which were mainly based on fluorophore- or biotin-labeled substrates toward the probing of carbohydrate−receptor recognitions.[6−11]

Indeed, carbohydrates are extraordinarily complex owing to their tremendous structural and especially configurational diversity. For example, glucose and galactose represent a pair of the simplest monosaccharide epimers that differ only in the C4 stereocontrol, whereas their biological characteristics are entirely different. Nature is exquisitely tuned to sense such a small configurational difference through specific molecular recognition of carbohydrate recognition domains (CRD), whereas artificial chemical probes that can reliably and quickly capture such nuances are still challenging.

Electrochemistry is known as a swift and sensitive analytical technology with facile and inexpensive instrumentations, which has been successfully employed in a multitude of wonderful biochemical studies including ion-channel recording,[12a−c] DNA

Received: November 22, 2010
Published: February 22, 2011

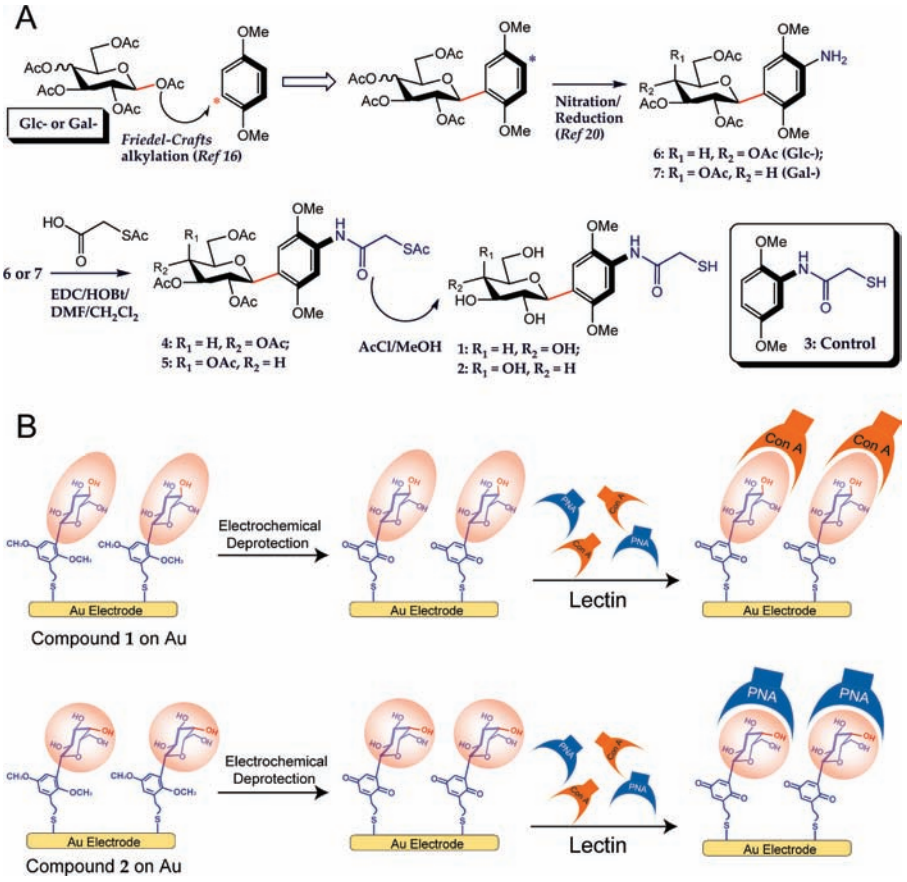

Figure 1. (A) Synthetic route of compounds **1** and **2**. (B) Fabrication of the electroactive sugar−quinone gold surface by the SAM technique, electrochemical deprotection, and the sensing for lectins.

recognition,[12d,13a,14a] single-nucleotide polymorphism (SNP) study,[13b] cancer biomarking,[14b] etc. Nevertheless, efforts that are devoted to the probing of specific carbohydrate−receptor interactions on the basis of electrochemically active sensors remain scant.[15] We have previously prepared a series of glucose−quinone or galactose−quinone hybrids with a short and solid *C*-glycosidic linkage that is resistant to acidic as well as enzymatic cleavage.[16] With these ideal features, we sought to investigate whether such quinonyl epimeric *C*-glycosides would potentially be utilized in electrochemical study.

The self-assembled monolayer (SAM) technique[17] has recently absorbed considerable interest as a potent complement for fabricating carbohydrate-coated surfaces that highly mimic the natural morphology of sugar chains pervaded on the cell surface,[18] offering reliable and presumable structure relationship toward multivalent carbohydrate−receptor interactions.[19] In view of such compelling merits, we were prompted to fabricate gold surface-attached SAMs that are electrochemically measurable based on epimeric monosaccharide−quinone hybrids.

In order to attach sugar−quinones on the gold surface, we initially synthesized aryl *C*-glycosides **1** and **2** (Figure 1A) with a sulfhydryl precursor. From amino *C*-glucosyl-1,4-dimethoxybenzene and *C*-galactosyl-1,4-dimethoxybenzene,[20] which were synthesized by our previous synthetic schemes involving the Friedel−Crafts alkylation[16] and a nitration/reduction sequence,[20] the peracetylated sulfhydryl aryl *C*-glycosides **4** and **5** were obtained via N-acylation. Successive deacetylation with AcCl gave the desired glycosides **1** and **2** with a free sulfhydryl anchor that can be coated on a gold electrode via the SAM technique. X-ray photoelectron spectroscopy (XPS) was sequentially conducted for confirming the SAM formation, followed by electrochemical deprotection,[21] which eventually generated the surface-confined hydroquinone/quinone redox couple.

Next, as illustrated in Figure 1B, the applicability of our uniquely characterized monosaccharide−quinone SAMs was preliminarily attempted toward the probing of specific carbohydrate−lectin[22] interactions via electrochemistry. Interestingly, upon addition of the specific lectin to corresponding monosaccharide−quinone SAM, i.e., Con A to the glucosyl SAM and PNA to the galactosyl SAM, a remarkably decreased peak current was observed in its cyclic voltammetry (CV) plots, whereas the addition of the same lectins in a reverse fashion gave much minor current variations. Differential pulse voltammetry (DPV) successively enabled a more detailed investigation on such glycosyl SAM−lectin interactions, demonstrating that the current decrease of the sugar−quinone SAMs is proportional to the lectin concentrations increased. Furthermore, a panel of nonspecific lectins was assayed on both glycosyl SAMs for further ascertaining their biospecificity via DPV, which resulted in minor changes in peak current. These results have supported the notion of proposing our uniquely characterized sugar−quinone SAMs as novel electrochemical probes for the detection of specific sugar−receptor interactions.

■ EXPERIMENTAL SECTION

Materials. Concanavalin A (Con A), (peanut agglutinin) PNA, *Pisum satiwum* agglutinin (PSA), soybean agglutinin (SBA), *Ulex*

dx.doi.org/10.1021/ja110478j |*J. Am. Chem. Soc.* 2011, 133, 3649–3657

europeaus agglutinin (UEA-I), wheat germ agglutinin (WGA), *Datura stramonium* agglutinin (DSA), and *Sambucus nigra* agglutinin (SNA) were purchased from Sigma-Aldrich or Shanghai Shrek Biotechnology Co., Ltd. All reagents and materials are of analytical grade, and solvents were purified by standard procedures. All solutions for analytical study were prepared with deionized water obtained with a Milli-Q System (Billerica, MA, U.S.A.).

General Procedure for the N-Acylation. To a solution of **6** or **7** (1 equiv)[20] and 2-(acetylthio)acetic acid (3 equiv) in dry DMF (5 mL) and CH_2Cl_2 (0.5 mL) were added 1-ethyl-3-(3-dimethylaminopropyl) carbodiimide hydrochloride (EDC, 3 equiv) and 1-hydroxbenzotriazole (HOBt, 2 equiv) at 0 °C, then the mixture was allowed to r.t., stirring for 6 h. Then, solvent was removed in vacuum and the residue washed successively with aqueous HCl (1 N), saturated aqueous $NaHCO_3$, and brine and extracted with CH_2Cl_2. The combined organic layers were dried over $MgSO_4$, filtered, concentrated in vacuum to dryness, and then purified by column chromatography.

*Tetra-O-acetyl-glucopyranosyl-S-(2-((2,5-dimethoxyphenyl)amino)-2-oxoethyl)ethanethioate (**4**).* From compound **6** (161 mg, 0.3 mmol) and 2-(acetylthio)acetic acid (142 mg, 1.1 mmol), EDC (191 mg, 1.0 mmol), HOBt (93 mg, 0.7 mmol), column chromatography (EtOAc/petroleum ether, 1:1) afforded compound **4** (161 mg, 80%) as a light yellow solid; R_f = 0.4 (EtOAc/petroleum ether, 1:1); $[\alpha]_D = -0.9$ (c = 0.1, CH_2Cl_2). ^{1}H NMR (400 MHz, $CDCl_3$): δ = 8.53 (s, 1H), 8.08 (s, 1H), 6.89 (s, 1H), 5.36 (t, J = 9.2 Hz, 1H), 5.26 (t, J = 10.0 Hz, 1H), 5.22 (t, J = 10.0 Hz, 1H), 4.96 (d, J = 10.0 Hz, 1H), 4.27 (dd, J = 4.8, 12.4 Hz, 1H), 4.13 (dd, J = 2.0, 12.4 Hz, 1H), 3.87 (s, 3H), 3.86−3.83 (m, 1H), 3.80 (s, 3H), 3.76−3.66 (m, 2H), 2.45, 2.07, 2.06, 2.00, 1.79 (5s, 15H). ^{13}C NMR (100 MHz, $CDCl_3$): δ = 195.2, 170.7, 170.2, 169.6, 169.3, 166.2, 151.5, 142.1, 128.6, 118.9, 109.6, 103.6, 76.1, 74.5, 73.0, 72.0, 68.9, 62.5, 56.4 (1), 56.4 (2), 34.4, 30.2, 20.8, 20.6, 20.4. HR-ESI-MS (m/z): calcd for $[M + Na]^+$ 622.1570, found 622.1570.

*Tetra-O-acetyl-galactopyranosyl-S-(2-((2,5-dimethoxyphenyl)amino)-2-oxoethyl)ethanethioate (**5**).* From compound **7** (181 mg, 0.4 mmol) and 2-(acetylthio)acetic acid (169 mg, 1.3 mmol), EDC (225 mg, 1.2 mmol), HOBt (104 mg, 0.8 mmol), column chromatography (EtOAc/petroleum ether, 1:1) afforded compound **5** (172 mg, 77%) as a yellow solid; R_f = 0.3 (EtOAc/petroleum ether, 1:1); $[\alpha]_D = +76.0$ (c = 0.1, CH_2Cl_2). ^{1}H NMR (400 MHz, $CDCl_3$): δ = 8.55 (s, 1H), 8.09 (s, 1H), 6.95 (s, 1H), 5.52 (dd, J = 0.4, 3.2 Hz, 1H), 5.43 (t, J = 10.0 Hz, 1H), 5.21 (dd, J = 3.2, 10.0 Hz, 1H), 4.93 (d, J = 10.0 Hz, 1H), 4.20−4.06 (m, 3H), 3.89 (s, 3H), 3.81 (s, 3H), 3.76−3.66 (m, 2H), 2.45, 2.21, 2.03, 1.99, 1.80 (5s, 15H). ^{13}C NMR (100 MHz, $CDCl_3$): δ = 195.2, 170.4, 170.3, 170.1, 169.4, 166.2, 151.5, 142.1, 128.6, 119.3, 110.0, 103.6, 74.7, 73.5, 72.4, 69.4, 67.9, 61.6, 56.5, 56.3, 34.3, 30.1, 20.8, 20.7, 20.6, 20.5. HR-ESI-MS (m/z): calcd for $[M + Na]^+$ 622.1570, found 622.1573.

General Procedure for the Deacetylation. To a solution of **4** or **5** (100.0 mg, 0.17 mmol) in MeOH (5 mL) was slowly added AcCl (1.5 equiv.), stirring at reflux for 10 h. Then, the solvent was removed in vacuum and the residue directly purified by column chromatography to afford compound **1** and by reversed-phase high-performance liquid chromatography (HPLC) to afford compound **2**, respectively.

*N-(2,5-Dimethoxy-4-((2S,3R,4R,5S,6R)-3,4,5-trihydroxy-6-(hydroxymethyl)tetrahydro-2H-pyran-2-yl)phenyl)-2-mercaptoacetamide (**1**).* From compound **4**, column chromatography (DCM/MeOH, 6:1) afforded compound **1** as a reddish-brown solid (20 mg, 32%); R_f = 0.5 (DCM/MeOH, 4:1); $[\alpha]_D = +9.1$ (c = 0.1, MeOH). ^{1}H NMR (400 MHz, D_2O): δ = 6.93 (s, 1H), 6.56 (s, 1H), 4.58 (d, J = 9.6 Hz, 1H), 3.78 (dd, J = 1.6, 13.6 Hz, 1H), 3.76 (s, 3H), 3.70 (s, 3H), 3.68 (dd, J = 2.8, 7.6 Hz, 1H), 3.65 (d, J = 9.2 Hz, 1H), 3.60−3.55 (m, 2H), 3.58 (q, J = 7.2 Hz, 2H), 3.49−3.46 (m, 2H). ^{13}C NMR (100 MHz, D_2O): δ = 164.9, 152.8, 142.2, 137.5, 115.8, 112.6, 102.0, 80.1, 77.6, 75.3, 73.0, 69.8, 60.8, 56.9, 56.8, 36.9. HR-ESI-MS: calcd for $[M - 74 + Na]^+$ 338.1216, found 338.1237.

*N-(2,5-Dimethoxy-4-((2S,3R,4R,5R,6R)-3,4,5-trihydroxy-6-(hydroxymethyl)tetrahydro-2H-pyran-2-yl)phenyl)-2-mercaptoacetamide (**2**).* From compound **5**, reversed-phase HPLC (t_R = 9.4 min over 76 min of 85% methanol/water, purity 100%) afforded compound **1** as a reddish-white solid (5 mg, 8%). ^{1}H NMR (400 MHz, D_2O): δ = 8.27 (s, 1H), 7.63 (s, 1H), 7.23 (s, 1H), 4.66 (d, J = 10.0 Hz, 1H), 4.01 (d, J = 2.8 Hz, 1H), 3.84 (t, J = 9.2 Hz, 1H), 3.82 (s, 3H), 3.76 (s, 3H), 3.78−3.75 (m, 2H), 3.72 (dd, J = 2.4, 9.6 Hz, 2H), 3.68 (d, J = 10.0 Hz, 2H). HR-ESI-MS: calcd for $[M - H]^-$ 388.1066, found 388.1065.

NMR, Optical Rotation, HPLC, and HRMS. ^{1}H and ^{13}C NMR spectra of compounds **1**, **2**, **4**, and **5** (shown in the Supporting Information) were recorded on a Bruker AM-400 spectrometer in $CDCl_3$ or D_2O solutions using tetramethylsilane as an internal standard. Optical rotations were measured using a Perkin-Elmer 241 polarimeter at room temperature and a 10 cm 1 mL cell. HPLC purification was carried out on a Yilite P230II HPLC system. High-resolution mass spectra (HRMS) were recorded on a Waters LCT Premier XE spectrometer instrument using standard conditions (ESI, 70 eV).

Monolayer Formation. The electrode surface was polished on an emery paper and alumina slurry until a mirror-like surface was obtained, followed by sonication in ethanolic solution at least for 2 min. Electropolishing was then conducted using consecutive cyclic voltammograms in 0.5 mol/L sulfuric acid and potential scanning between 0.5 and 1.5 V versus saturated calomel electrode (SCE) until a typical voltammogram for gold was obtained. The SAMs were simply formed by immersing a clean gold electrode in an ethanolic solution of 1 mM ethanethioates (**1**, **2**, or **3**) for a period of 36 h.

XPS. XPS spectra were obtained on an Axis-165 X-ray photoelectron spectrometer (Kratos Analytical) using a monochromatic Al Kα X-ray source (1486.7 eV). Survey spectra (0−1100 eV) were taken at constant analyzer pass energy of 160 eV, and all high-resolution spectra for C_{1s}, N_{1s}, O_{1s}, S_{2p}, and Au_{4f} were acquired with a pass energy of 20 eV, a step of 0.1 eV, and a dwell time of 200 ms. The takeoff angle between the film surface and the photoelectron energy analyzer was 90°. The typical operating pressure was around 5×10^{-10} Torr in the analysis chamber. Various scan numbers were carried out for the different elements to obtain the high signal-to-noise ratio. The binding energies were referenced to the $Au_{4f7/2}$ at 84.0 eV, and peaks were fitted using the publicly available XPSPEAK v. 4.1. The Shirley function was used as a background and Gaussian−Lorentzian cross-products used to fit the individual peaks. The samples for XPS measurements were prepared from the SAMs containing compounds **1**, **2**, or **3** on gold-coated silicon chips (5 mm × 5 mm size, West Chester, PA U.S.A.). Before the chips were incubated in deaerated solutions of the SAMs, the chips were carefully precleaned by soaking in hot Piranha solution (H_2SO_4/H_2O_2 = 3:1) for 10 min (***Caution!*** *Piranha solution should be handled with extreme care and should never be stored in a closed container. It is a very strong oxidant and reacts violently with most organic materials*) and then sonicated in Millipore H_2O for three times.

Electrochemical Deprotection, CV, and DPV. All electrochemical experiments were conducted with a computer-controlled CHI 660 electrochemical station (Chenhua Co. Ltd., Shanghai, China). Working electrodes were 3 mm diameter disk gold (Au) electrodes, used in conjunction with a Pt auxiliary electrode, and a Ag/AgCl wire pseudoreference electrode worked as the reference electrode. Electrochemical deprotection of SAMs containing compounds **1**−**3** was realized by scanning the potential between −0.3 and 0.9 V with a scan rate of 100 mV/s in 0.1 M H_2SO_4 after the formation of the corresponding SAMs on the Au electrode. After electrochemical deprotection of SAMs **1** and **2** on the gold surface, the electrode was incubated for 5 min in the presence of various lectins in PBS (pH = 7.0) to determine the sugar−lectin interactions. All voltammetric experiments were performed after deaeration for 5 min with nitrogen. DPV measurement was recorded with increasing amounts of lectins ranging from 0 to 10 μM, driving

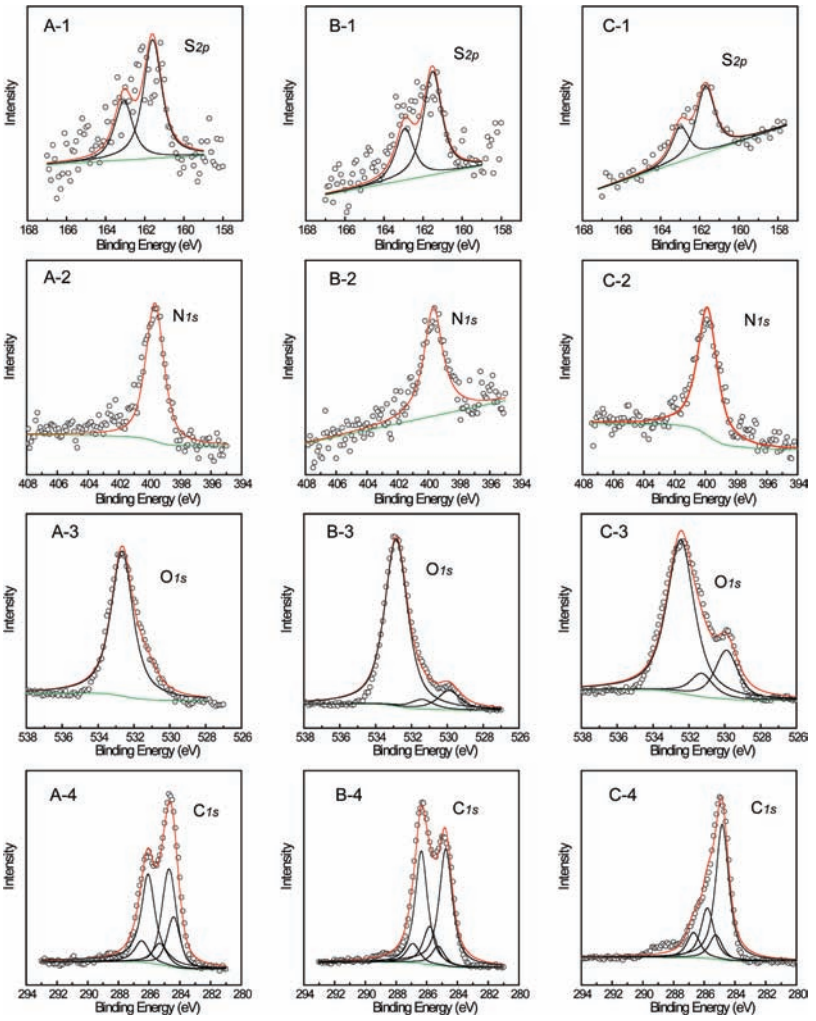

Figure 2. High-resolution XPS spectra of S_{2p}, N_{1s}, O_{1s}, and C_{1s} for SAM **1** (A-1−A-4), SAM **2** (B-1−B-4), and SAM **3** (C-1−C-4) on a gold surface. Open circles stand for experimental raw data, red solid lines are for the total fits, black lines are for the component-fitted peaks, and green lines are for the baselines.

potential from −0.3 to 0.4 V with a pulse amplitude of 50 mV and a sample pulse width of 100 ms.

RESULTS AND DISCUSSION

Synthesis of Sulfhydryl Aryl *C*-Glycosides. To fabricate glycosylated SAMs on the gold surface, we chose to employ a sulfide linker which has been shown to efficiently immobilize various sugar moieties onto a gold surface.[19,24] As shown in Figure 1A, amino *C*-glucosyl-dimethoxybenzene **6** and amino *C*-galactosyl-dimethoxybenzene **7** were first obtained via the Lewis acid promoted Friedel−Crafts alkylation[16] and a nitration/reduction sequence.[20] Then, the N-acylation of compounds **6** and **7** with commercially available 2-(acetylthio)acetic acid in the presence of EDC and HOBt afforded sulfides **4** and **5**, respectively. Notably, an amide linkage was chosen to couple aryl *C*-glycosides with the sulfhydryl precursor due to its ability to form hydrogen bonds within the monolayer matrix, thus reinforcing the stability and rigidness of the surface-attached SAM.[19,25] Successive deacetylation with AcCl and purification by column chromatography or reversed-phase HPLC yielded the desired glycosides **1** and **2** containing a free sulfhydryl anchor, respectively. Glucosyl and galactosyl derivatives which only differ in their C4 configuration were prepared in this study since they uniquely interact with corresponding lectins, i.e., glucose−Con A and galactose−PNA. Such specific epimeric carbohydrate−protein interactions were presumed discriminable via electrochemistry.

SAM Formation and XPS Characterization. With the sulfhydryl *C*-glycosyl derivatives **1** and **2** in hand, we attempted to fabricate the glycosylated gold surface by using the known sulfhydryl 1,4-dimethoxybenzene (Figure 1A, **3**)[23] as a control. The formation of SAMs containing, respectively, compounds **1**−**3** on the gold surface was simply realized by immersing a clean gold electrode in an ethanolic solution of 1 mM **1**, **2**, or **3** for a period of 36 h.

The XPS that represents a quantitative and surface-sensitive analytical technique to verify the chemical composition of the SAM samples[26] was used to substantiate the SAM formation. In order to prevent the excess contamination by carbon and oxygen species, the gold surface has been carefully precleaned with fresh Piranha solution prior to incubation in deaerated solutions containing compounds **1**, **2**, and **3**. The high-resolution XPS spectra then permitted direct quantification of the chemical

Table 1. Binding Energy (BE, eV) of O_{1s} and C_{1s} of Compound 1-, 2-, and 3-Coated SAMs in the XPS Spectra

O_{1s} spectra				C_{1s} spectra			
	BE (ratio)[a]				BE (ratio)		
component	SAM **1**	SAM **2**	SAM **3**	component	SAM **1**	SAM **2**	SAM **3**
methoxyl-O	n/A[b]	529.9 (2)	529.9 (2)	benzene ring-C	284.7 (6)	284.7 (6)	284.7 (6)
carbonyl-O	n/A	531.4 (1)	531.3 (1)	S−C	285.3 (1)	285.3 (1)	285.3 (1)
sugar-O	532.7	532.9 (16)	n/A	methoxyl-C	284.4 (2)	285.8 (2)	285.8 (2)
water-O	532.7	532.9 (16)	532.5 (7)	sugar-C	286.1 (6)	286.4 (6)	n/A
				carbonyl-C	286.5 (1)	286.8 (1)	286.7 (1)

[a] The values in parentheses are ratios of peak areas calculated from given XPS spectrum. [b] n/A means "not available".

species to provide detailed information for the composition of the SAMs **1**−**3** on the gold surface.

As shown in Figure 2A−C, the XPS peaks of S_{2p}, N_{1s}, C_{1s}, and O_{1s} for each compound were fitted and deconvoluted to give the chemical shift data of the components within the coated molecules, respectively. Two dominant peaks located at 161.7 and 162.9 eV with an area ratio of 2:1 and a peak separation of 1.2 eV were observed in the S_{2p} spectra (Figure 2, parts A-1, B-1, and C-1) of SAMs **1**−**3**, which could be assigned to the S atom bound on the gold surface.[27] From their N_{1s} spectra as shown in Figure 2, parts A-2, B-2, and C-2, the single peak centered at 399.8 eV without difference in chemical shifts indicates the presence of amide-N on the surface of each SAM.

The O_{1s} spectrum of SAM **3** (Figure 2C-3) then gave three obvious peaks centered at 529.9, 531.3, and 532.5 eV, attributable to the methoxyl-O, carbonyl-O, and the oxygen atom of water molecules adsorbed on the surface (Table 1, O_{1s}, SAM **3**) with a peak area ratio of 2:1:7. In contrast, the O_{1s} spectra of the SAMs **1** and **2** that contain epimeric monosaccharides showed a remarkable difference. As shown in Figure 2A-3, for the SAM that contains the galactoside **2**, its methoxyl-O and carbonyl-O peaks were similarly observed at 529.9 and 531.4 eV, respectively (Table 1, O_{1s}, SAM **2**), with a peak area ratio of 2:1. Another peak centered at 532.9 eV seems to contain both the sugar-O and the water-O peaks, which are proportionally larger than that of the water-O peak shown for the control SAM **3** (Figure 2C-3). However, only one broadened peak centered at 532.7 eV was fittable in Figure 2A-3 for the SAM containing the glucoside **1**, which could probably ascribe to the chemical shift of its methoxyl-O peak to the higher binding energy field, leading to the superposition of the methoxyl-O, carbonyl-O, sugar-O, and the water-O peaks (Table 1, O_{1s}, SAM **1**).

Interestingly, an obvious peak shift was also observed in the C_{1s} spectrum of SAM **1**. By first comparing the C_{1s} spectra between SAMs **2** (Figure 2B-4) and **3** (Figure 2C-4), their benzene ring-C, S−C, methoxyl-C, and carbonyl-C peaks were similarly centered at 284.7, 285.3, 285.8, and 286.8 eV (286.7 eV for SAM **3**), whereas an additional peak appeared at 286.4 eV exclusively for the galactosyl SAM **2**, assignable to the sugar-C (Table 1, C_{1s}, SAMs **2** and **3**). The peak ratios of both SAMs (**2** and **3**) are in the correct proportion, listed in the parentheses of Table 1, C_{1s}, SAMs **2** and **3**. In stark contrast, despite that the benzene-C (284.7 eV), S−C (285.3 eV), sugar-C (286.1 eV), and carbonyl-C (286.5 eV) peaks of the glucosyl SAM **1** (Figure 2A-4) were positioned likewise, an apparent chemical shift of its methoxyl-C peak (284.4 eV) to the lower energy binding field by 1.4 eV was clearly observed comparing with that of the galactosyl SAM **2** (285.8 eV, Table 1, C_{1s}, SAMs **1** and **2**).

A plausible explanation of the chemical shifts for the glucosyl SAM **1** was then tentatively proposed. Since the common carbon and oxygen atom peaks are almost identically located in their corresponding spectra for the galactosyl SAM **2** and the control SAM **3** that lacks the saccharide moiety, the varied binding energy (BE) of the glucosyl SAM **1** could be probably caused by its stronger intermolecular hydrogen-bonding interactions with the water molecule. Apparently, the only difference between the glucosyl and the galactosyl SAM lies in the C4 configuration with the former owning a C4 equatorial OH group and the latter bearing a C4 axial OH group. As a consequence, the C4 axial hydroxyl bond that is closer to the methoxyl group of the aglycon with a β-configuration might have performed as a shutter to further prevent the generation of intermolecular hydrogen bonds with the water molecule. In contrary, the equatorial bond of the glucosyl moiety that is spatially more distant from this methoxyl-O might result in a spatial gap for intermolecular hydrogen bonds between water and the methoxyl-O on the benzene ring. The electron cloud density of this oxygen atom would thus be decreased, which could result in its chemical shift toward the high binding energy field, whereas the electron cloud density of the methoxyl-C covalently attached with this oxygen atom might have been increased for charge balance, leading to its chemical shift toward the low binding energy field.[28] Notably, such difference caused by epimeric identity between SAMs **1** and **2** is also reflected in their chemical reactivity during the electrochemical deprotection process described below.

Consequently, the XPS analysis confirmed that compounds **1**−**3** have been successfully chemisorbed on the gold electrode surface via self-assembly.

Electrochemical Deprotection. Electrochemical deprotection of the XPS-confirmed methylated (hydroxy)quinone SAMs **1**−**3** was successively proceeded to generate the hydroquinone/quinone redox couple.[21b] In Figure 3, CVs recorded at 100 mV/s between −0.3 and 0.9 V versus Ag/AgCl in 0.1 M H_2SO_4 are shown for each SAM. The CV of the control SAM (**3**, Figure 3C-1) showed no obvious redox peak in the first scan segment, whereas an oxidation peak at E_{pa} = 0.357 V and a reduction peak at E_{pc} = 0.283 V were observed with successive scans. Further increase in scan number led to consecutive increase of peak currents but slight shifts of peak potentials. Eventually, the redox peak current tended to stabilize on the electrode surface after 10 continuous scans with the anodic and cathodic peaks being symmetric and broad and a full width at half-height (fwhh) equal to 0.1 V.

dx.doi.org/10.1021/ja110478j |*J. Am. Chem. Soc.* 2011, 133, 3649–3657

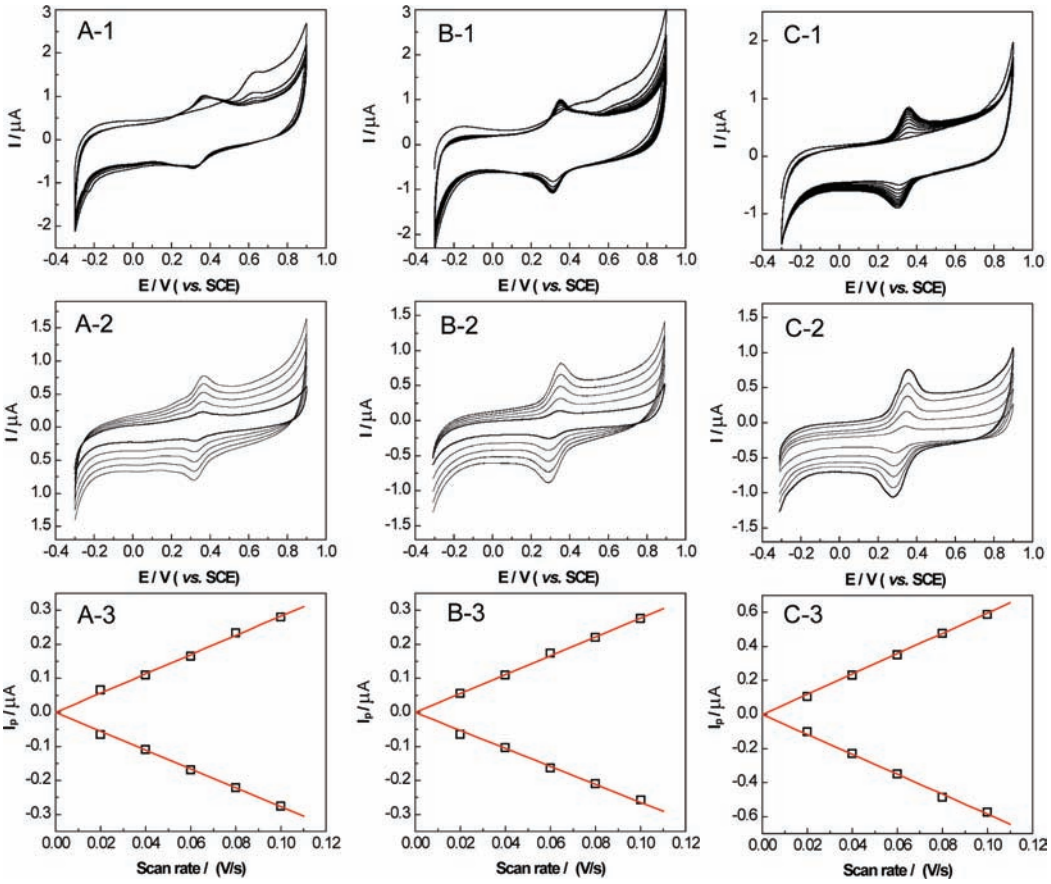

Figure 3. Cyclic voltammograms (CVs) of SAMs on gold electrodes created from the practically deprotected forms of compounds **1** (A), **2** (B), and **3** (C). The CVs were recorded with 10 continuing scans at a scan rate of 100 mV/s in 0.1 M H_2SO_4 as illustrated in panels A-1, B-1, and C-1. The CVs were recorded in 0.1 M H_2SO_4 at scan rates of 0.020, 0.040, 0.060, 0.080, and 0.100 V/s as illustrated in panels A-2, B-2, and C-2. Peak currents of SAMs **1**, **2**, and **3** on gold electrodes, I_p, as a function of scan rate, ν, is illustrated in panels A-3, B-3, and C-3. All first scans were initiated in the positive direction from −0.3 V.

For the SAMs **1** (Figure 3A-1) and **2** (Figure 3B-1) that contain epimeric monosaccharides, new irreversible oxidation peaks were apparently observed at E_{pa} = 0.617 V (SAM **1**) and 0.641 V (SAM **2**) in the initial scan with the rapid generation of new redox couples centered at E_f (formal potentials, calculated by taking the average of the anodic and cathodic peak potentials) = 0.333 V (SAM **1**) and 0.340 V (SAM **2**), respectively, only after the second scan. With increased scans, both SAMs displayed slightly increased peak currents, suggesting a much easier deprotection process comparing to that of the control SAM **3**. This demonstrates that the monosaccharide moiety closely conjugated with the dimethoxybenzene may accelerate the electrochemical deprotection process. In addition, the glucosyl SAM **1** is comparatively easier to be deprotected compared with the galactosyl SAM **2** as its irreversible oxidation peak could be more facilely generated by the initial scan (Figure 3, part A-1 vs part B-1). This could be similarly caused by the axial C4 hydroxyl group of the galactoside that is spatially closer to the β-aglycon, impeding the formation of the hydroxyquinone/quinone redox couple in a certain extent.[29] The peak separation between the oxidation and reduction peaks of both SAMs **1** (Figure 3A-1) and **2** (Figure 3A-2) is small, suggesting that the electron-transfer kinetics between the glycosyl quinone and the electrode is a fast process. Furthermore, both redox peaks in the CVs of SAMs **1** and **2** are symmetric and broad with fwhh's equal to 0.125 V (SAM **1**) and 0.126 V (SAM **2**), respectively.

After electrochemical deprotection, the CVs of each SAM in 0.1 M H_2SO_4 as a function of scan rate were recorded for characterizing their corresponding monolayer properties. The diagrams outlined in Figure 3, parts A-3 (SAM **1**), B-3 (SAM **2**), and 3C-3 (SAM **3**), revealed that the currents of all redox peaks increased while the scan rate increased with no significant shifts in peak potentials. Furthermore, as illustrated in these diagrams, both anodic and cathodic peak currents for hydroquinone/quinone redox couples of each SAM scaled linearly with the scan rates ranging from 0.020 to 1.000 V/s (Figure 3, parts A-2,3, B-2,3, and C-2,3, only shows their CV characteristics with scan rates from 0.020 to 0.100 V/s; for full characteristics with scan rates from 0.020 to 1.000 V/s see Supporting Information Figure S-1), indicating that the oxidation and reduction processes of the quinones are surface-controlled.

To characterize the monolayer properties of each SAM, the surface coverage (Γ, mol/cm^2) was calculated by integrating the area of the anodic and cathodic peaks. Taken into account the electrochemical roughness factor (R_f = 1.42 ± 0.11), which was assessed by CV between −0.1 and 1.5 V versus SCE at 100 mV/s in freshly prepared 0.1 M H_2SO_4, the coverage (Γ) for SAM **1** is assigned to 3.91(0.28) × 10^{-11} mol/cm^2, and those for SAMs **2**

dx.doi.org/10.1021/ja110478j |*J. Am. Chem. Soc.* 2011, 133, 3649–3657

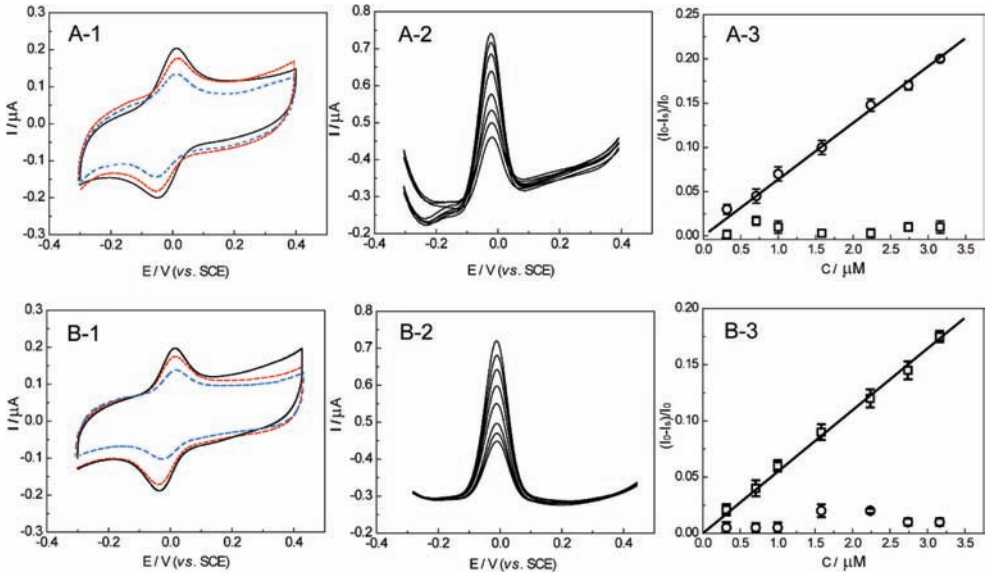

Figure 4. CVs of (A-1) SAM **1** upon addition of PNA (4 μM, red dot line) and Con A (4 μM, blue dot line) at a scan rate of 40 mV/s and (B-1) SAM **2** upon addition of Con A (4 μM, red dot line) and PNA (4 μM, blue dot line) at a scan rate of 40 mV/s. DPV response of (A-2) SAM **1** upon the addition of various concentrations of Con A ranging from 0.1 to 10 μM and (B-2) SAM **2** upon the addition of various concentrations of PNA ranging from 0.1 to 10 μM. Monitoring the change in DPV current between background and sample as a function of lectin concentrations: (A-3) Con A (○) and PNA (□); (B-3) Con A (□) and PNA (○).

and **3** are 4.66(0.31) $\times$ 10^{-11} mol/cm^2 and 9.47(0.45) $\times$ 10^{-11} mol/cm^2, respectively. These values are smaller than the typical coverage found for the hydroquinone/quinone redox couple with bridges containing alkane thiols (Γ = 3.2−5.7 $\times$ 10^{-10} mol/cm^2),[30] which could be caused by the existence of the bulky benzo(hydro)quinone and sugar moieties that furnish excessive spatial hindrance. Meanwhile, the surface coverage per molecule on the surface of the three SAMs was assessed, which equals to 0.24 $\pm$ 0.02 nm^{-2} for glucosyl SAM **1**, 0.28 $\pm$ 0.2 nm^{-2} for galactosyl SAM **2**, and 0.57 $\pm$ 0.3 nm^{-2} for sugar-free SAM **3**. The successively calculated footprint of one molecule on a gold electrode for each SAM was assigned to 4.2 $\pm$ 0.3 nm^2 for **1**, 3.6 $\pm$ 0.2 nm^2 for **2**, and 1.7 $\pm$ 0.2 nm^2 for **3**.

Indeed, the electrochemical approach fulfilled in the present case has overcome the synthetic inconvenience and greatly consumed the excessive purification effort, directly and facilely providing the desired electroactive monosaccharide−quinone SAMs for further study.

Electrochemical Probing of Specific Carbohydrate−Lectin Interactions. With the accomplished electrochemical monosaccharide−quinone SAMs, we sought to attempt preliminarily its applicability toward the detection of specific epimeric carbohydrate−protein interactions. Naturally occurring Con A and PNA that are known to possess, respectively, specific glucose and galactose recognition domains were used for this study.[22]

The CVs of monosaccharide−quinone SAMs **1** and **2** in the absence (in black) or in the presence (in red or blue) of lectins were first detected, shown in Figure 4. As exhibited in both parts A-1 and B-1 of Figure 4, when a lectin that bears the specific CRD was added to the corresponding SAM, i.e., Con A to the glucosyl SAM **1** and PNA to the galactosyl SAM **2**, the resulting peak current decreased remarkably (in blue), whereas minor changes in peak current (in red) were observed while the lectins were added in a reverse fashion, i.e., PNA to **1** and Con A to **2**. Interestingly, the peak potentials as well as the peak breadth of both SAMs did not change upon the addition of the specific lectin, indicating that the electrochemical kinetics was not influenced. As it is reported that the peripheric enzymatic surface adjacent to the CRD of natural lectins may interact with hydrophobic groups,[5] the decreased current could consequently be ascribed to the binding of lectin to both monosaccharide and quinonyl moieties.[15] When the lectin binds simultaneously to the sugar−quinone hybrid in the system, the corresponding electron-transfer process of the SAM would be blocked, sequentially leading to the decrease of peak current. Moreover, the very small peak current decrease afforded by the glycosyl SAM−nonspecific lectin mixture might be most likely caused by the partial interaction of the quinone moiety with such lectin.

Next, for investigating the monosaccharide−quinone SAM−lectin interactions in a more detailed way, we recorded DPVs of SAMs **1** and **2** with increasing amounts of lectins ranging from 0 to 10 μM in 0.1 M PBS solution at pH = 7.0. Clearly, as shown in Figure 4, parts A-2 and B-2, upon the addition of gradually increased specific lectin, i.e., Con A to SAM **1** and PNA to SAM **2**, the corresponding peak current gradually decreased with no obvious peak shift or variation in breadth. This further demonstrates that the decrease of peak current of both SAMs is concentration-dependent. Eventually, while the highest concentration (10 μM) of Con A was added to SAM **1**, the corresponding peak current decreased by 68%, whereas the addition of the same amount of PNA to SAM **2** led to the decrease of peak current by 40%. As shown in Figure 4, parts A-3 (**1**) and B-3 (**2**), the percentage of decreased current I_d=(I_0 − I_s)/I_0 was subsequently plotted versus the lectin concentrations ranging from 0.1 to 10 μM where the I_d is fractional decrease in current, I_0 is the current with no added lectin, and I_s is the current with added lectin. The resulting linear relationship represents the specific monosaccharide−lectin interactions, i.e., Con A to SAM **1** (r^2 = 0.9984) and PNA to SAM **2** (r^2 = 0.9990), whereas the addition of nonspecific lectins to the same SAMs leads to very minor

dx.doi.org/10.1021/ja110478j |*J. Am. Chem. Soc.* 2011, 133, 3649–3657

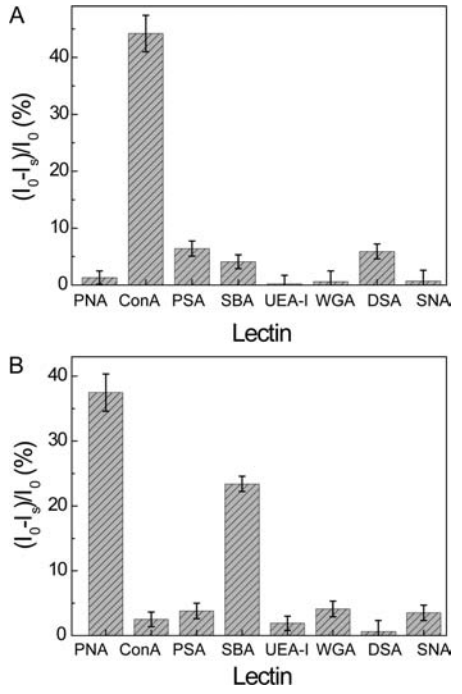

Figure 5. Percentages (%) of peak current decrease of (A) SAM **1** and (B) SAM **2** upon addition of 7 μM of various specific or nonspecific lectins where I_0 is the current with no added lectin and I_s is the current with added lectin.

changes in I_d value with increasing concentrations. The detection limit of both SAMs was calculated to be 75 nM ($S/\sigma_{b1} = 3$, where σ_{b1} is the standard deviation of the peak current obtained in the absence of lectin).

Additionally, in an attempt to further ascertain their biospecificity, a panel of nonspecific lectins that are known to recognize specifically other natural monosaccharide subunits including PSA (mannose-specific), SBA (*N*-acetyl-galactosamine-specific), UEA-I (fucose-specific), WGA (*N*-acetyl-glucosamine- and sialic acid-specific), DSA (*N*-acetyl-glucosamine-specific), and SNA (sialic acid-specific) was assayed on both glycosyl SAMs **1** and **2** via DPV. To our delight, with the addition of 7 μM Con A and PNA to, respectively, the corresponding SAMs **1** and **2**, remarkable peak current decreases (44% for SAM **1** and 37% for SAM **2**) were similarly observed, shown in Figure 5 and Supporting Information Figure S-2 (complete DPV plots of SAMs **1** and **2** upon addition of various lectins). In stark contrast, while the selected nonspecific lectins such as PSA, UEA-1, WGA, DSA, and SBA (to SAM **1** only) were added at the same concentration (7 μM) to the SAMs, very minor peak current changes were displayed, with the addition of SBA to SAM **2** as an exception. Notably, it is known that SBA binds more specifically to *N*-acetyl-D-galactosamine, whereas the galactose unit may also be recognized by its CRD, however, with weaker binding affinity. Hence, we would ascribe the relatively less significant peak current decrease (24%) of the galactosyl SAM **2** in the presence of SBA than that (37%) in the presence of PNA to its comparatively lesser binding specificity to the former than to the latter.

These data have positively established our uniquely constructed sugar−quinone SAMs containing natural monosaccharide epimers applicable toward the accurate probing of specific sugar−protein interactions via electrochemistry.

CONCLUSIONS

In summary, we have successfully realized in this study the fabrication of novel gold surface-coated epimeric monosaccharide−quinone SAMs by taking advantage of simple synthetic progressions of our previously synthesized aryl *C*-glycosides in conjunction with the subsequent SAM technique and electrochemical deprotection. Their epimeric identity was concomitantly reflected in both the XPS spectra and the electrochemical deprotection process. The afforded electroactive SAMs containing monosaccharide epimers were then demonstrated efficacious toward the sensitive probing of specific epimeric sugar−lectin interactions (i.e., glucose−Con A, galactose−PNA) with weaker or very minor responses to the addition of a panel of less specific and nonspecific lectins via CV or DPV.

Indeed, since there develops increasing interest as well as urgent need in the elaboration of carbohydrate-related biological and pathological processes by probing the specific carbohydrate−receptor recognitions, our newly fabricated sugar−quinone SAMs might be desirable as an ingenious probe toward such studies with the quick and sensitive electrochemistry. Moreover, on the basis of the presently established systematic method for constructing surface-attached sugar−quinone hybrids, numerous other electrochemically active sugar SAMs containing diverse biologically important carbohydrate entities could be developed and collected to further fabricate sugar microarrays[18] for efficiently monitoring specific carbohydrate−receptor interactions that are naturally involved in the intricate cellular processes, in the near future. This unique electrochemical platform would presumably facilitate the better understanding of the "glycomics" as well as the development of early-state disease diagnosis.

ASSOCIATED CONTENT

Supporting Information. Figures S-1 and S-2, original NMR spectra of compounds **1**, **2**, **4**, and **5**, and the HR-ESI-MS spectrum of compound **2**. This material is available free of charge via the Internet at http://pubs.acs.org.

AUTHOR INFORMATION

Corresponding Author
ytlong@ecust.edu.cn

ACKNOWLEDGMENT

We thank the National Natural Science Foundation of China (Grant No. 20876045, 91027035), Ministry of Health (Grant 2009 ZX 10004-301), Shanghai Science and Technology Community (No. 10410702700), and the Fundamental Research Funds for the Central Universities (No. WK1013002). Y.-T. Long is supported by the Program for Professor of Special Appointment (Eastern Scholar) at Shanghai Institutions of Higher Learning. X.-P. He also gratefully acknowledges the French Embassy in China for a doctorate fellowship and his French advisor Professor Juan Xie in ENS Cachan.

REFERENCES

(1) Bertozzi, C. R.; Kiessling, L. L. *Science* **2001**, *291*, 2357–2364.
(2) Raman, R.; Raguram, S.; Venkataraman, G.; Paulson, J. C. *Nat. Methods* **2005**, *2*, 718–824.

(3) Fukuda, M.; Hindsgaul, O. *Molecular and Cellular Glycobiology*; Oxford University Press: Oxford, U.K., 2000.
(4) Seeberger, P. H. *Nature* **2005**, *437*, 1239.
(5) Lis, H.; Sharon, N. *Chem. Rev.* **1998**, *98*, 637–674.
(6) Murthy, B. N.; Voelcker, N. H.; Jayaraman, N. *Glycobiology* **2006**, *16*, 822–832.
(7) (a) Liang, P. H.; Wang, S. H.; Wong, C. H. *J. Am. Chem. Soc.* **2007**, *129*, 11177–11184. (b) Kuno, A.; Uchiyama, N.; Koseki-Kuno, S.; Ebe, Y.; Takashima, S.; Yamada, M.; Hirabayashi, J. *Nat. Methods* **2005**, *2*, 851–856.
(8) (a) Disney, M. D.; Zhang, J.; Swager, T. M.; Seeberger, P. H. *J. Am. Chem. Soc.* **2004**, *126*, 13343–13346. (b) Dai, Z.; Kawde, A.-N.; Xiang, Y.; La Belle, J. T.; Gerlach, J.; Bhavanandan, V. P.; Joshi, L.; Wang, J. *J. Am. Chem. Soc.* **2006**, *128*, 10018–10019. (c) Munoz, E. M.; Correa, J.; Fernandez-Megia, E.; Riguera, R. *J. Am. Chem. Soc.* **2009**, *131*, 17765–11167.
(9) (a) Ricard-Blum, S.; Peel, L. L.; Ruggiero, F.; Freeman, N. J. *Anal. Biochem.* **2006**, *352*, 252–259. (b) Wu, J. H.; Singh, T.; Herp, A.; Wu, A. M. *Biochimie* **2006**, *88*, 201–217. (c) Pei, Y.; Yu, H.; Pei, Z.; Theurer, M.; Ammer, C.; Andre, S.; Gabius, H. J.; Ramstrom, O. *Anal. Chem.* **2007**, *79*, 6897–6902.
(10) Jelinek, R.; Kolusheva, S. *Chem. Rev.* **2004**, *104*, 5987–6015.
(11) (a) Scrafton, D. K.; Taylor, J. E.; Mahon, M. F.; Fossey, J. S.; James, T. D. *J. Org. Chem.* **2008**, *73*, 2871–2874. (b) Zhang, X.; Chi, L.; Ji, S.; Wu, Y.; Song, P.; Han, K.; Guo, H.; James, T. D.; Zhao, J. *J. Am. Chem. Soc.* **2009**, *131*, 17452–17463.
(12) (a) White, R. J.; Ervin, E. N.; Yang, T.; Chen, X.; Daniel, S.; Cremer, P. S.; White, H. S. *J. Am. Chem. Soc.* **2007**, *129*, 11766–11775. (b) Ervin, E. N.; White, R. J.; White, H. S. *Anal. Chem.* **2009**, *81*, 533–537. (c) Schibel, A. E. P.; Edwards, T.; Kawano, R.; Lan, W.; White, H. S. *Anal. Chem.* **2010**, *82*, 7259–7266. (d) Lathrop, D. K.; Ervin, E. N.; Barrall, G. A.; Keehan, M. G.; Kawano, R.; Krupka, M. A.; White, H. S.; Hibbs, A. H. *J. Am. Chem. Soc.* **2010**, *132*, 1878–1885.
(13) (a) Erickson, D.; Liu, X.; Krull, U.; Li, D. *Anal. Chem.* **2004**, *76*, 7269–7277. (b) Erickson, D.; Liu, X.; Venditti, R.; Li, D.; Krull, U. J. *Anal. Chem.* **2005**, *77*, 4000–4007.
(14) (a) Zhang, J.; Lao, R.; Song, S.; Yan, Z.; Fan, C. *Anal. Chem.* **2008**, *80*, 9029–9033. (b) Du, D.; Zou, Z.; Shin, Y.; Wang, J.; Wu, H.; Engelhard, M. H.; Liu, J.; Aksay, I. A.; Lin, Y. *Anal. Chem.* **2010**, *82*, 2989–2995.
(15) (a) Sugawara, K.; Kuramitz, H.; Kaneko, T.; Hoshi, S.; Akatsuka, K.; Tanaka, S. *Anal. Sci.* **2001**, *17*, 21–25. (b) Sugawara, K.; Shirotori, T.; Hirabayashi, G.; Kuramitz, H.; Kaneko, T.; Tanaka, S. *J. Electroanal. Chem.* **2004**, *568*, 7–12. (c) Sugawara, K.; Hirabayashi, G.; Kamiya, N.; Kuramitz, H. *Talanta* **2006**, *68*, 1176–1181. (d) Casas-Solvas, J. M.; Ortiz-Salmerón, E.; Gracía-Fuentes, L.; Vargas-Berenguel, A. *Org. Biomol. Chem.* **2008**, *6*, 4230–4235. (e) Casas-Solvas, J. M.; Ortiz-Salmerón, E.; Giménez-Martínez, J. J.; Gracía-Fuentes, L.; Capitán-Vallvey, L. F.; Santoyo-González, F.; Vargas-Berenguel, A. *Chem.—Eur. J.* **2009**, *15*, 710–725.
(16) (a) Praly, J. P.; He, L.; Qin, B. B.; Tanoh, M.; Chen, G.-R. *Tetrahedron Lett.* **2005**, *46*, 7081–7085. (b) He, L.; Zhang, Y. Z.; Tanoh, M.; Chen, G. R.; Praly, J. P.; Chrysina, E. D.; Tiraidis, C.; Kosmopoulou, M.; Leonidas, D. D.; Oikonomakos, N. G. *Eur. J. Org. Chem.* **2007**, 596–606.
(17) (a) Schreiber, F. *J. Phys.: Condens. Matter* **2004**, *16*, R881. (b) Chaki, N. K.; Vijayamohanan, K. *Biosens. Bioelectron.* **2002**, *17*, 1.
(18) (a) Feizi, T.; Fazio, F.; Chai, W.; Wong, C. H. *Curr. Opin. Struct. Biol.* **2003**, *13*, 637–645. (b) Wu, C. Y.; Liang, P. H.; Wong, C. H. *Org. Biomol. Chem.* **2009**, *7*, 2247–2254.
(19) (a) Yonzon, C. R.; Jeoung, E.; Zou, S.; Schatz, G. C.; Mrksich, M.; Van Duyne, R. P. *J. Am. Chem. Soc.* **2004**, *126*, 12669–12676. (b) Zhang, Y.; Luo, S. Z.; Tang, Y. J.; Yu, L.; Hou, K. Y.; Cheng, J. P.; Zeng, X. Q.; Wang, G. P. *Anal. Chem.* **2006**, *78*, 2001–2008.
(20) Zhang, Y. Z.; Aouadi, K.; Chen, G.-R.; Praly, J. P. *Synthesis* **2007**, *22*, 3473–3488.
(21) (a) Finklea, H. O. In *Encyclopedia of Analytical Chemistry*; Meyers, R. A., Ed.; John Wiley & Sons Ltd.: Chichester, U.K., 2000; pp 1−26. (b) Trammell, S. A.; Moore, M.; Schull, T. L.; Lebedev, N. *J. Electroanal. Chem.* **2009**, *628*, 125–133.
(22) Sharon, N.; Lis, H. *Lectins*, 2nd ed.; Kluwer Academic: Dordrecht, The Netherlands, 2003.
(23) Martin, D. F. *J. Am. Chem. Soc.* **1961**, *83*, 1076–1078.
(24) Smith, E. A.; Thomas, W. D.; Kiessling, L. L.; Corn, R. M. *J. Am. Chem. Soc.* **2003**, *125*, 6140–6148.
(25) (a) Clegg, R. S.; Hutchison, J. E. *J. Am. Chem. Soc.* **1999**, *121*, 5319–5327. (b) Valiokas, R.; Svedhem, S.; Svensson, S. C. T.; Liedberg, B. *Langmuir* **1999**, *15*, 3390–3394.
(26) (a) Laibinis, P. E.; Whitesides, G. M.; Allara, D. L.; Tao, Y.-T.; Parikh, A. N.; Nuzzo, R. G. *J. Am. Chem. Soc.* **1991**, *113*, 7152–7167. (b) Sun, F.; Castner, D. G.; Mao, G.; Mckeown, P.; Grainger, D. W. *J. Am. Chem. Soc.* **1996**, *118*, 1856–1866. (c) Evans, S. D.; Goppert-Beraducci, K. E.; Urankar, E.; Gerenser, L. J.; Ulman, A.; Snyder, R. G. *Langmuir* **1991**, *7*, 2700–2709. (d) Whelan, C. M.; Smyth, M. R.; Barnes, C. J.; Brown, N. M. D.; Anderson, C. A. *Appl. Surf. Sci.* **1998**, *134*, 144–158.
(27) (a) Castner, D. G.; Hinds, K.; Grainger, D. W. *Langmuir* **1996**, *12*, 5083–5086. (b) Ishida, T.; Yamamoto, S.; Mizutani, W.; Motomatsu, M.; Tokumoto, H.; Hokari, H.; Azehara, H.; Fujihira, M. *Langmuir* **1997**, *13*, 3261–3265.
(28) Kerber, S. J.; Bruckner, J. J.; Wozniak, K.; Seal, S.; Hardcastle, S.; Barr, T. L. *J. Vac. Sci. Technol., A* **1996**, *14*, 1314–1320.
(29) Gómez, M.; González, F. J.; González, I. *J. Electroanal. Chem.* **2005**, *578*, 193–202.
(30) Hong, H. G.; Park, W. *Langmuir* **2001**, *17*, 2485–2492.